LA-UR-99-5961
Approved for public release;
distribution is unlimited.

Title: **COLD DEMONSTRATION OF NON-TRADITIONAL *IN-SITU* VITRIFICATION (NTISV) AT LOS ALAMOS NATIONAL LABORATORY ON A SIMULATED ADSORPTION BED**

Author(s): Thomas Hartmann

Submitted to:

http://lib-www.lanl.gov/la-pubs/00796563.pdf

COLD DEMONSTRATION OF NON-TRADITIONAL *IN-SITU* VITRIFICATION (NTISV) AT LOS ALAMOS NATIONAL LABORATORY ON A SIMULATED ADSORPTION BED

Thomas HARTMANN
Environmental Science and Waste Technology Division, Los Alamos National Laboratory, Los Alamos, NM 87545, USA, hartmann@lanl.gov

ABSTRACT

A cold test demonstration of the Geosafe® Non-Traditional *In-Situ* Vitrification technology (NTISV) was performed at a simulated adsorption bed by using commercial-scale equipment. A successful demonstration of NTISV at Los Alamos National Laboratory (LANL) is expected to provide a useful technology for remediation needs of EM-40 in the U.S. Department of Energy (DOT) complex on legacy buried waste containing organics and radionuclides in geological environments. Therefore, a simulated test bed including surrogates was prepared to evaluate the impact this technology has on immobilizing radionuclides. The total volume of the cold demonstration vitrification was 3.1 m x 4.6 m x 4.9 m resulting in 176,667 kg of glass or glassy constituents. A drill core sample was removed from the glass monolith and divided into 13 samples to gain spatial (vertical) information about (a) vitrification progress, (b) phase distribution, and (c) element distribution. Based upon optical microscopy, least square and Rietveld refinement of the X-ray diffraction data, the phase constitution was determined and a temperature profile estimated. The glass compositions as well as the concentrations of surrogates and trace metals were analyzed by using X-ray fluorescence Analysis (XRF), Electron-beam Microprobe Analysis (EMPA), and Scanning Electron Microscopy (SEM). In the main melting zone, in the depth range 3.7 m to 6.3 m, NTISV successfully vitrified the geological formation (Bandelier Tuff, Unit 2/3 of Tshirege) and convert it mainly into 98-99 wt.-% silicate-based glass and 1-2 wt.-% iron-based metal inclusions. Within this zone the glass compositions have been found to be nearly constant and the surrogate elements (cerium and cesium) are distributed homogeneously.

INTRODUCTION

A cold test demonstration of the Geosafe Non-Traditional in-situ Vitrification technology (NTISV) was performed at a simulated adsorption bed by using Geosafe's commercial-scale equipment. Between 1945 and 1961, three former adsorption beds received effluent from a nuclear laundry and are now contaminated with a number of radionuclides. A successful demonstration of NTISV at LANL is expected to provide a useful technology for remediation needs on legacy buried waste containing organics and radionuclides in geological environments. Therefore, a simulated adsorption bed including surrogates was prepared to evaluate the impact of this technology on immobilizing radionuclides. The surrogates (6.5-kg Cs_2CO_3 and 30-kg CeO_2) were placed on the floor of the adsorption bed. The total volume of the vitrified tuff after cold demonstration was estimated to be 3.1 m x 4.6 m x 4.9 m (10 ft x15 ft x 16 ft) resulting in 67.95 m^3 or 176,667 kg of glass or glassy constituents. If NTISV is capable of providing perfect homogeneous element distribution within this estimated glass monolith, the surrogate inventory should increase the background concentrations up to 28.7 mg/kg in Cs and 138.2 mg/kg in Ce within the glass. The background element concentrations

have been found to be 2 to 3 mg/kg Cs and 111 mg/kg Ce [1]. In this work, results of phase distribution and element distribution as a function of depth are presented.

EXPERIMENTAL

A drill core was removed from the glass monolith, which represents the vitrified material and the amount of glass-forming oxides, as well as the surrogate charge. This drill core was divided into 13 samples (Table 1) which were analyzed to gain spatial (vertical) information about (a) vitrification progress, (b) phase distribution, and (c) element distribution by following methods:

- X-ray diffraction (XRD, Scintag XDS 2000) and least square refinement (Rietveld refinement [2]) to determine the phase constitution, as well as the vitrification progress.
- Optical Polarization Microscopy (Zeiss) to determine homogeneity, and the presence of residuals
- X-ray fluorescence (XRF, Rigaku 3064) to analyze glass composition, as well as the distribution of surrogates and trace metals
- Electron-beam Microprobe Analysis (EMPA, Cameca SX50 operated at 15 kV, 30 nA) to analyze glass matrices and metal inclusions with high spatial resolution.
- Scanning Electron Microscopy (SEM, Noran Instruments ADEM) to characterize the nature of metal inclusions.

RESULTS AND DISCUSSION

As a result of studies by Rietveld refinement on X-ray diffraction data, and optical microscopy, three different phase constitutional zones were distinguished as a function of depth (Table 1, Fig.1).

Table 1: Samples analyzed by XRD, XRF, EMPA, SEM, and optical microscopy

Upper Zone		**Main Melting Zone**		**Lower Zone**	
Sample Name	**Depth Below Surface**	**Sample Name**	**Depth Below Surface**	**Sample Name**	**Depth Below Surface**
TH1-10 6608	1.83 m to 3.05m 6 ft to 10 ft	**TH4-15.9** 6611	4.7 m to 4.85 m 15.5 ft to 15.9 ft	**TH11-20.5** 6618	6.25 m 20.5 ft
TH2-12 6609	3.2 m to 3.66 m 10,5 ft to 12 ft	**TH5-16** 6612	4.85 m to 4.9 m 15.9 ft to 16.0 ft	**TH12-21.5** 6619	6.55 m 21.5 ft
TH3-15 6610	3.66 m to 4.6 m 12 ft to 15 ft	**TH6-16.8** 6613	4.9 m to 5.1 m 16.0 ft to 16.8 ft	**TH13-22.5** 6620	6.55 m to 7.0 m 21.5 ft to 22.8 ft
		TH7-17 6614	4.9 m to 5.2 m 16.8 ft to 17.0 ft		
		TH8-18 6615	5.18 m to 5.5 m 17.0 ft to 18.0 ft		
		TH9-18.9 6616	5.5 m to 5.8 m 18.0 ft to 18.9 ft		
		TH10-20 6617	5.8 m to 6.25 m 18.9 ft to 20.5 ft		

In the depth range between 1.8 m and 4.6 m (upper zone) vitrification of the simulated adsorption bed progresses from no significant vitrification (TH1-10) to nearly complete

vitrification (TH3-15). In the main melting zone between 4.7 m and 6.25 m temperatures of 1700°C and higher were achieved. As a consequence, the simulated adsorption bed is fully vitrified. Unfortunately, redox conditions caused by the technological set-up (graphite electrodes, graphite starter plates, no oxidizing agent) are not in favor to reach optimum solubilities of transition metals within the silicate-based glass melt. As a result, a liquid-liquid miscibility gap between the silicate-based melt and an iron-metal-based melt occurs. The metal–based melt tend to accumulate to bigger aggregates in order to minimize its surface energy, and in a second stage to segregate and to deposit at the bottom of the melt which is caused by its about 3 times higher density. Fortunately, the high viscosity of the melt caused by high SiO_2 content prevents significant segregation of the metal inclusions within the temperature and time range applied in the cold test experiment. In the depth range between 5.2 m and 6.25 m small amounts (1-2 wt.-%) of the high-temperature modification of cristobalite (SiO_2) were detected. The presence of this SiO_2 polymorph indicates a temperature regime of 1470°C to 1700°C. Below 6.25 m (lower zone) the temperature decreases rapidly to about 1470°C to 870°C. This temperature range is not sufficient enough for a complete vitrification of the simulated adsorption bed. As a result, the glassy content decreases to about 30 wt.-% and no vitrification products could be found in depths of 6.6 m or below. At a 7-m depth, residual low-cristobalite, as a frozen leftover from the devitrification in the geological formation (Bandelier tuff) is present, which is a good indication that the temperature did not exceed 800°C.

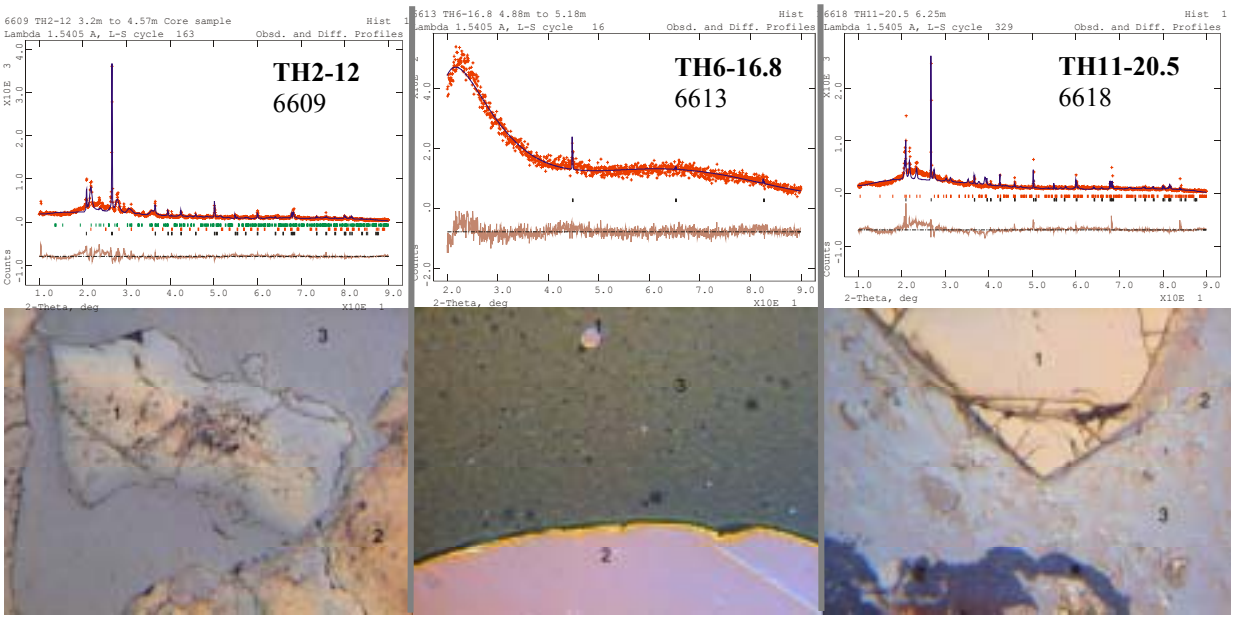

Upper Zone
1: residual quartz, low-cristobalite
2: feldspar (sanidine)
3: glass phase

Main Melting Zone
1: metal inclusion
2: agglomerated metal inclusion
3: glass phase

Lower Zone
1: quartz, tridymite
2: sanidine (nepheline-type)
3: glass phase

Figure 1: Rietveld refinement and optical microscopy of a representative sample from each zone

Based upon least square refinement of the X-ray diffraction data results, the phase constitution can be determined and a temperature profile estimated (Fig.2).

X-ray fluorescence analysis (XRF) was used to analyze the major oxide content of the samples (Fig. 3), and the distribution of the surrogates (Ce, Cs) (Fig. 5). XRF was also used to determine the concentrations of trace metals (Ba, Zr, Sr, Rb, Zn, Nb, Y, V, Cr, and Ni) within the drill core samples. Electron-beam microprobe analysis (EMPA) was used for quantitatively analyzing glass matrices (Fig. 4) and metal inclusions.

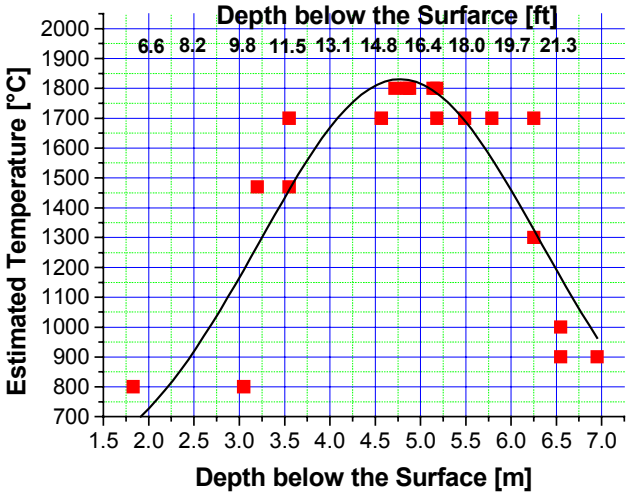

Figure 2: Estimated temperature profile as a function of depth based on the determined phase constitutions

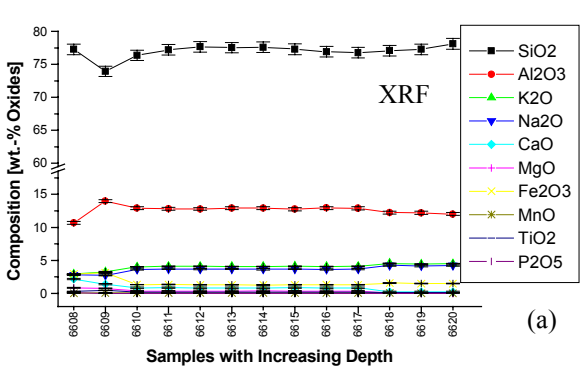

Figure 3: Sample composition measured by XRF

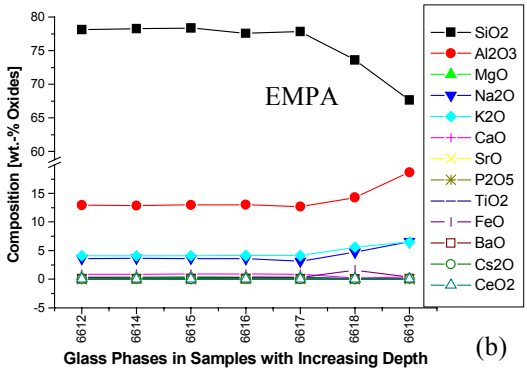

Figure 4: Glass compositions measured by EMPA

Glass compositions in the main melting zone (6610 to 6617) were found to be similar. The amount of the main glass-former SiO_2 is very consistent and varies between 76.4 (±0.8) wt.-% and 76.8 (±0.8) wt.-%. This high and homogeneous content in SiO_2 provides the glass monolith with excellent properties as an actinide host. Furthermore, the low (10 wt.-%) content of pure network modifier (K_2O, Na_2O, CaO, MgO) is allowing a perfectly linkage between the SiO_2 tetrahedron within the glass structure and in all three dimensions. This strong linkage between the structural elements within the glass structure will result in good corrosion resistance under severe weathering condition. Surface-related samples (e.g. 6609) are

influenced by the infiltration of weathering products. The sample composition of 6608 is affected by the heat cover (sand, gravel, cobble) and the SiO_2 content is shifted towards higher amounts, from estimated 70-71 wt.-% to 77.3 (±0.8) wt.-% SiO_2. Excluding impacts of the experimental set-up, higher surface concentrations of Al_2O_3, CaO, MgO, Fe_2O_3, TiO_2 and P_2O_5 were measured, while the SiO_2, K_2O and Na_2O contents were lower. The NTISV technology is capable to provide appropriate convection and intermixing within the melt, and the resulting glass compositions were found to be between tuff composition and the composition oft the near surface area. Below 6.25 m vitrification in the NTISV cold demonstration was not complete, which is indicated by lower SiO_2 concentrations (6618, 6619). The temperatures in depths below 20.5 ft were too low to completely melt the tuff, and residual SiO_2-modifications remained.

In the group of trace metals (Ba, Zr, Sr, Rb, Zn, Nb, Y, V, Cr) the Zn concentration does reflect the behavior of volatile or semi-volatile metals in this cold test vitrification experiment (Fig.5). Zinc is volatile under the temperature condition of the main melting zone and is not becoming part of the glass structure. Zinc oxide easily reduces under the redox conditions in the experiment and metallic Zn is transported apart from the heat source and condensed in a lower temperature regime of about 907°C. The colder area surrounding the heat source is highly enriched with zinc, indicating how the other volatile metals of this group (Cd, Hg) will act.

The distributions of cerium and cesium in the cold test experiment are strongly related (Fig.6). The surrogates placed, at 1.8-m depth, are enriched in the main melting zone at constant concentrations. The homogeneous surrogate distributions within the main melting zone demonstrate that intermixing caused by convection is appropriate. In the cold demonstration experiment the cerium background concentration (tuff) was increased from 95(±7) mg/kg to 212(±7) mg/kg in the main melting zone. The cesium concentration ranged from 18(±6) mg/kg (tuff) to 47(±6) mg/kg in the main melting zone. Because of the semi-volatile character of cesium, the Cs-concentration in the tuff formation close to the melting zone was enriched (18 mg/kg) and above the expected cesium background concentration of 2-3 mg/kg. In a first approximation, the cesium concentration profile apart from the heat source can be estimated and a cesium background concentration of 3(±1) mg/kg will be reached in a 7.3-m to 7.35-m depth, about 1.30 m below the main melting zone. The lateral spread of cesium will certainly exceed this 1.30-m vertical spread, since volatile metals try to move to lower surrounding pressure.

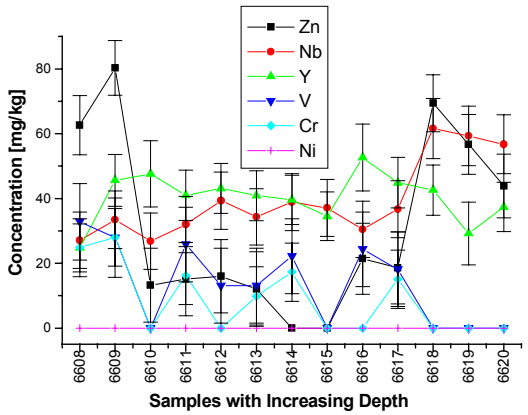

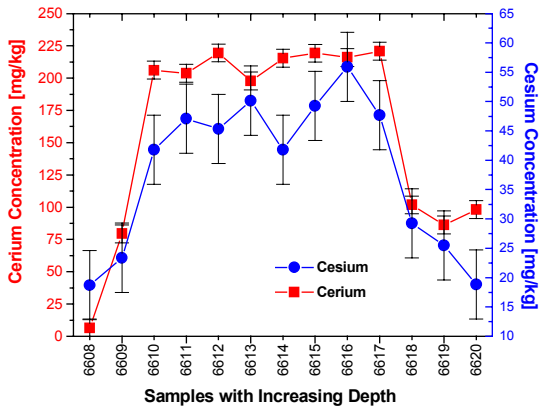

Figure 5: Zinc distribution within the experiment among other trace metals

Figure 6: Cerium and Cesium accumulation in the main melting zone

Element compositions of metal inclusions were under investigation by using electron-beam microprobe analysis (EMPA) as well as scanning electron microscopy (SEM). The metal inclusions mainly consist of iron, and a α-Fe(Si) phase ($Fe_{94}Si_5P_1$) with 2-3 wt.-% silicon, and a phosphorus enriched iron-based phases ($Fe_{96}P_4$ to $Fe_{80}P_{20}$) were identified. The metal inclusions are ideal host for non-ferrous metal as opposed to rare earth elements, and enrichments with niobium, titanium, vanadium, and nickel were measured. The surrogate concentrations in metal inclusions are similar or below the concentrations in the glass matrices. As far as the complete system is understood, the formation of metal inclusion causes only marginal negative effects on the hydrodynamic behavior of the glass monolith under weathering conditions.

CONCLUSION

The deployment of Geosafe's Non Traditional *In-Situ* Vitrification (NTISV) on Bandelier tuff (Unit 2/3 of the Tshirege member) was successful for fully vitrifying the geological formation in a depth range of 3.7 m to 6.25 m. The energy transfer into this main melting zone was sufficient to achieve temperatures of 1700°C and higher and to initiate appropriate material flow and convection for obtaining a very homogeneous product. As a result, the amount of primary glass-former SiO_2 is consistently high. Since the content of pure network modifier (K_2O, Na_2O, CaO, MgO) is low (about 10 wt.-%), a perfect three-dimensional linkage of the SiO_2 tetrahedron in the glass structure will be achieved. These high ratios of glass former to network modifier allow high solubilities of radionuclides within the glass structure and causes high corrosion resistance under severe weathering conditions. Unfortunately, the redox conditions in this experiment, caused by the technological set-up do not favor optimum solubilities of transition metals within the silicate-based glass melt. Since in this experiment the iron inventory is low (1-2 wt.-%), the melt in the technological process was never in danger of freezing. However, there is a potential risk for freezing the vitrification process if the total iron-metal inventory exceeds 10-15 wt.-%. In these cases oxidizing agents should be introduced. Metal inclusions are not suitable as actinide hosts, and the concentrations of the surrogates were similar or below the concentrations within the glass matrices. The hydrodynamic performance of the monolith will be slightly diminished by the presence of these metal inclusions, but will still be appropriate to stabilize the expected radioactive content in the material disposal areas (MDAs) for a long period of time. The surrogates are nearly entirely enriched in the main melting zone exhibiting constant concentrations. The enrichment of these surrogate metals in the main melting zone strongly supports the deployment of the NTISV technology in plutonium contaminated sites, since the thermodynamic data for cerium and plutonium are very similar. Plutonium will also be enriched in the main melting zone where glass-forming conditions are optimal. The cesium distribution indicated, that minor amounts of semi-volatile radionuclides and transition metals will be driven off the heat source and will migrate into surrounding non-vitrified rock formations. This potential relocation of hazardous material can not be avoided by changing glass composition or redox conditions and should be further investigated and better understood.

ACKNOWLEDGMENTS

This research was sponsored by the US Department of Energy under the Program Code MR8A 0403 A186.

REFERENCES

[1] Geosafe Corporation, *Non-traditional in-situ vitrification at the Los Alamos National Laboratory- Cold demonstration report*, GSC report 363, 64 pages, 1999.

[2] A.C. Larson, R.B. Von Dreele, *General Structure Analysis System*, LA-UR-86-748, LANL report, Los Alamos National Laboratory, Los Alamos, NM, USA, 1986.